Doppler peaks in the angular power spectrum of the cosmic microwave background : a fingerprint of topological defects

Durrer, Ruth; Gangui, Alejandro; Sakellariadou, Mairi

How to cite

DURRER, Ruth, GANGUI, Alejandro, SAKELLARIADOU, Mairi. Doppler peaks in the angular power spectrum of the cosmic microwave background : a fingerprint of topological defects. In: Physical review letters, 1996, vol. 76, n° 4, p. 579–582. doi: 10.1103/PhysRevLett.76.579

This publication URL: https://archive-ouverte.unige.ch/unige:989
Publication DOI: 10.1103/PhysRevLett.76.579

Doppler Peaks in the Angular Power Spectrum of the Cosmic Microwave Background: A Fingerprint of Topological Defects.

Ruth Durrer*, Alejandro Gangui†‡ and Mairi Sakellariadou*

* *Université de Genève*
Département de Physique Théorique
4, quai E. Ansermet
CH-1211 Genève 4, Switzerland

† *SISSA – International School for Advanced Studies*
Strada Costiera 11, 34014 Trieste, Italy

‡ *ICTP – International Center for Theoretical Physics*
P. O. Box 586, 34100 Trieste, Italy

Abstract

The Doppler peaks (Sacharov peaks) in the angular power spectrum of the cosmic microwave background anisotropies, are mainly due to coherent oscillations in the baryon radiation plasma before recombination. Here we present a calculation of the Doppler peaks for perturbations induced by global textures and cold dark matter. We find that the height of the first Doppler peak is smaller than in standard cold dark matter models, and that its position is shifted to $\ell \sim 350$. We believe that our analysis can be easily extended to other types of global topological defects and general global scalar fields.

PACS numbers: 98.80-k 98.80.Hw 98.80C

Presently there are two main classes of models to explain the origin of large scale structure formation. Initial perturbations can either be due to quantum fluctuations of a scalar field during an inflationary era[1], or they may be seeded by topological defects formed during a symmetry breaking phase transition in the early universe[2]. The CMB anisotropies are a powerful tool to discriminate among these models by purely linear analysis. Usually CMB anisotropies are parameterized in terms of C_ℓ's, defined as the coefficients in the expansion of the angular correlation function

$$\langle \frac{\delta T}{T}(\mathbf{n}) \frac{\delta T}{T}(\mathbf{n}') \rangle \Big|_{(\mathbf{n}\cdot\mathbf{n}'=\cos\vartheta)} = \frac{1}{4\pi} \sum_\ell (2\ell+1) C_\ell P_\ell(\cos\vartheta).$$

For scale invariant spectra of perturbations $\ell(\ell+1)C_\ell$ is constant on large angular scales, say $\ell \lesssim 50$. Both inflation and topological defect models lead to approximately scale invariant spectra on large scales.

Large scale CMB anisotropies are mainly caused by inhomogeneities in the space-time geometry via the Sachs–Wolfe (SW) effect[3]. On smaller angular scales ($0.1^\circ \lesssim \theta \lesssim 2^\circ$) the dominant contribution comes from coherent oscillations in the baryon–radiation plasma prior to recombination. On even smaller scales the anisotropies are damped due to the finite thickness of the recombination shell, as well as by photon diffusion during recombination (Silk damping).

Disregarding Silk damping, gauge invariant linear perturbation analysis leads to[4]

$$\frac{\delta T}{T} = \left[-\frac{1}{4}D_g^{(r)} - V_j n^j - \Psi + \Phi\right]_i^f + \int_i^f (\Psi' - \Phi')d\tau \ , \tag{1}$$

where Φ and Ψ are quantities describing the perturbations in the geometry and $\mathbf{V}$ denotes the peculiar velocity of the baryon fluid with respect to the overall Friedmann expansion. $D_g^{(r)}$ specifies the intrinsic density fluctuation in the radiation fluid. There are several gauge invariant variables which describe density fluctuations; they all differ on super–horizon scales but coincide inside the horizon. Below we use another quantity, D_r, for the radiation density fluctuation. The variables $D_g^{(r)}$ and D_r are defined in Eq. (II.5.28b) and Eq. (II.5.27b) of ref. [5] respectively, for an arbitrary matter component α. Here $_r$ stands for the coupled baryon radiation fluid[1]. Since the coherent oscillations giving rise to the Doppler peaks act only on sub–horizon scales, the choice of this variable is irrelevant for our calculation.

Φ , Ψ and $D_g^{(r)}$ in Eq. (1) determine the anisotropies on large angular scales[2], and have been calculated for both inflation and defect models [6, 7, 8, 9]. Generically, a scale invariant spectrum is predicted and thus the SW calculations yield mainly a normalization for the different models. On the other hand the amplitude of the Doppler peak, which most probably will be measured in the near future, might be an important discriminating tool between them. In this *Letter* we present a computation for the Doppler contribution from global topological defects; in particular we perform our analysis for π_3–defects, textures [10], in a universe dominated by cold dark matter (CDM). We believe that our main conclusion remains valid for all global defects.

[1]Actually $D_r = (\delta\rho_r + \delta\rho_b)/(\rho_r + \rho_b)$ is not quite the variable for the temperature fluctuation, $\delta T/T = (1/4)\delta\rho_r/\rho_r$. A short calculation shows that D_r is about 5% smaller than $\delta\rho_r/\rho_r$.

[2]One might think that $D_g^{(r)}$ leads *just* to coherent oscillations of the baryon radiation fluid, but this is not the case. Note that, e.g., for adiabatic CDM models without source term one can derive $(1/4)D_g^{(r)} = -(5/3)\Psi$ on super–horizon scales. Since for CDM perturbations, $\Phi = -\Psi$ and $\Psi' \simeq 0$, the usual SW result $\delta T/T = (1/3)\Psi(\mathbf{x}_{rec}, t_{rec})$ is recovered. Neglecting $D_g^{(r)}$, the result would be 2Ψ and therefore wrong by a factor of 6!

The Doppler contribution to the CMB anisotropies is approximately given by[3]

$$\left[\frac{\delta T}{T}(\mathbf{x},\mathbf{n})\right]^{Doppler} \approx \frac{1}{4}D_r(\mathbf{x}_{rec},t_{rec}) + \mathbf{V}(\mathbf{x}_{rec},t_{rec})\cdot\mathbf{n}, \tag{2}$$

where $\mathbf{x}_{rec} = \mathbf{x} - \mathbf{n}t_0$. In the previous formula $\mathbf{n}$ denotes a direction in the sky and t is conformal time, with t_0 and t_{rec} the present and recombination times, respectively. Due to the inaccuracies mentioned in the previous footnotes, Eq. (2) tends to underestimate the amplitude of the first Doppler peak by up to 30%. On the other hand, we neglect Silk damping of perturbations, which leads to a slight overestimation. We thus are on the safe side, if we postulate that approximation (2) leads to an error of less than about 30% in the amplitude of the first Doppler peak and overestimates the value ℓ of its position by less than 10%. The nice feature of Eq. (2) is that we will need only one simple scalar component of the defect stress–energy tensor to evaluate it.

To determine D_r and $\mathbf{V}$ at t_{rec}, we consider a two–fluid system: baryons plus radiation, which prior to recombination are tightly coupled, and CDM. The evolution of the perturbation variables in a flat background, $\Omega = 1$, is described by[5]

$$\begin{aligned}
V_r' + \tfrac{a'}{a}V_r &= k\Psi + k\tfrac{c_s^2}{1+w}D_r \\
V_c' + \tfrac{a'}{a}V_c &= k\Psi \\
D_r' - 3w\tfrac{a'}{a}D_r &= (1+w)[3\tfrac{a'}{a}\Psi - 3\Phi' - kV_r - \tfrac{9}{2}\left(\tfrac{a'}{a}\right)^2 k^{-1}(1+\tfrac{w\rho_r}{\rho})V_r] \\
D_c' &= 3\tfrac{a'}{a}\Psi - 3\Phi' - kV_c - \tfrac{9}{2}\left(\tfrac{a'}{a}\right)^2 k^{-1}(1+\tfrac{w\rho_r}{\rho})V_c \ ,
\end{aligned} \tag{3}$$

where subscripts $_r$ and $_c$ denote the baryon–radiation plasma and CDM, respectively; D, V are density and velocity perturbations; $w = p_r/\rho_r$, $c_s^2 = p_r'/\rho_r'$ and $\rho = \rho_r + \rho_c$. The only place where the seeds enter this system is through the potentials Ψ and Φ. These potentials can be split into a part coming from standard matter and radiation, and a part due to the seeds, $\Psi = \Psi_{(c,r)} + \Psi_s$ and $\Phi = \Phi_{(c,r)} + \Phi_s$, where Ψ_s and Φ_s are determined by the energy momentum tensor of the seeds. In this way, the seed source terms will arise below[4].

From Eqs. (3) we derive two second order equations for D_r and D_c, namely

$$\begin{aligned}
D_r'' + \frac{a'}{a}[1 + 3c_s^2 - 6w + F^{-1}\rho_c]D_r' - \frac{a'}{a}\rho_c F^{-1}(1+w)D_c' \\
+4\pi G a^2[\rho_r(3w^2 - 8w + 6c_s^2 - 1) - 2F^{-1}w\rho_c(\rho_r + \rho_c) \\
+\rho_c(9c_s^2 - 7w) + \frac{k^2}{4\pi G a^2}c_s^2]D_r - 4\pi G a^2\rho_c(1+w)D_c &= (1+w)S \ ;
\end{aligned} \tag{4}$$

[3]In principle this Doppler term has to be added to the SW contribution. But the SW contribution decays on subhorizon scales (like ℓ^{-2}). At horizon scales, especially the last term in Eq. (1), the integrated Sachs–Wolfe (ISW) effect, can be important. At $\ell = 200$ it contributes about 30% to the angular power spectrum for standard adiabatic CDM. Neglecting it, slightly shifts the first Doppler peak to smaller angular scales, $\ell \approx 220$, as we have found by testing our code for the standard adiabatic CDM model. Since we will find here, that the first Doppler peak is lower than in this model, the ISW contribution might be higher. However, as we shall see below, the peak is at $\ell = 365$. Therefore we expect a suppression by $(365/200)^2 \approx 3$, so that the ISW contribution to the peak is probably not much higher. We also neglect the contribution of the neutrino fluctuations. But since even the dark matter fluctuations yield only about 20% of the gravitational potential, we expect the neutrino fluctuations, which for standard models contribute about 20%, to be considerably smaller.

$$D_c'' + \frac{a'}{a}[1 + (1+w)F^{-1}\rho_r(1+3c_s^2)]D_c' - \frac{a'}{a}(1+3c_s^2)F^{-1}\rho_r D_r'$$
$$-4\pi G a^2 \rho_c D_c - 4\pi G a^2 \rho_r (1+3c_s^2)[1 - 2(\rho_r+\rho_c)F^{-1}w]D_r \;=\; S \;, \quad (5)$$

where $F \equiv k^2(12\pi G a^2)^{-1} + \rho_r(1+w) + \rho_c$ and S denotes a source term, which in general is given by $S = 4\pi G a^2(\rho + 3p)^{seed}$. In our case, where the seed is described by a global scalar field ϕ, we have $S = 8\pi G(\phi')^2$. From numerical simulations one finds that the average of $|\phi'|^2$ over a shell of radius k, can be modeled during the matter dominated era by[9]

$$\langle|\phi'|^2\rangle(k,t) \;=\; \frac{\frac{1}{2}A\eta^2}{\sqrt{t}[1+\alpha(kt)+\beta(kt)^2]}, \quad (6)$$

with η denoting the symmetry breaking scale of the phase transition leading to texture formation. The parameters in (6) are $A \sim 3.3$, $\alpha \sim -0.7/(2\pi)$ and $\beta \sim 0.7/(2\pi)^2$. On super–horizon scales, where the source term is important, this fit is accurate to about 10%. As we argue later, analytical estimates support this finding. On small scales the accuracy reduces to a factor of 2. By using this fit[4] in the calculation of D_r and D_c from Eqs. (4), (5) we effectively neglect the time evolution of phases of $(\phi')^2$; the incoherent evolution of these phases may smear out subsequent Doppler peaks[11], but will not affect substantially the height of the first peak.

From D_r and D_r' we calculate the Doppler contribution to the C_ℓ's according to

$$C_\ell = \frac{2}{\pi}\int dk \left[\frac{k^2}{16}|D_r(k,t_{rec})|^2 j_\ell^2(kt_0) + (1+w)^{-2}|D_r'(k,t_{rec})|^2 (j_\ell'(kt_0))^2\right], \quad (7)$$

where j_ℓ denotes the spherical Bessel function of order ℓ and j_ℓ' stands for its derivative with respect to the argument. The angular power spectrum $\ell(\ell+1)C_\ell$ yields the Doppler peaks.

In order to solve Eqs. (4), (5) we need to specify initial conditions. For a given scale k we choose the initial time t_{in} such that the perturbation is super–horizon and the universe is radiation dominated. In this limit the evolution equations reduce to

$$D_r'' - \frac{2}{t^2}D_r \;=\; \frac{4}{3}\frac{A\epsilon}{\sqrt{t}} \;; \quad (8)$$

$$D_c'' + \frac{3}{t}D_c' - \frac{3}{2t}D_r' - \frac{3}{2t^2}D_r \;=\; \frac{A\epsilon}{\sqrt{t}} \;, \quad (9)$$

with particular solutions

$$D_r \;=\; -\frac{16}{15}\epsilon A t^{3/2} \;;\; D_c \;=\; -\frac{4}{7}\epsilon A t^{3/2} \;. \quad (10)$$

In the above equations we have introduced $\epsilon \equiv 4\pi G\eta^2$, the only free parameter in the model. We consider perturbations seeded by the texture field, and therefore it is incorrect to add a homogeneous growing mode to the above solutions. With these initial conditions, Eqs. (4), (5) are easily integrated numerically, leading to the spectra for $D_r(k,t_{rec})$ and $D_r'(k,t_{rec})$ [*see*, Fig. 1].

[4] Our fit is not valid in the radiation dominated era. There, logarithmic corrections or a different power law might have to be applied. Since the relevant scales enter the horizon roughly during the matter–radiation transition, this renders the amplitude of the corresponding fluctuations somewhat uncertain.

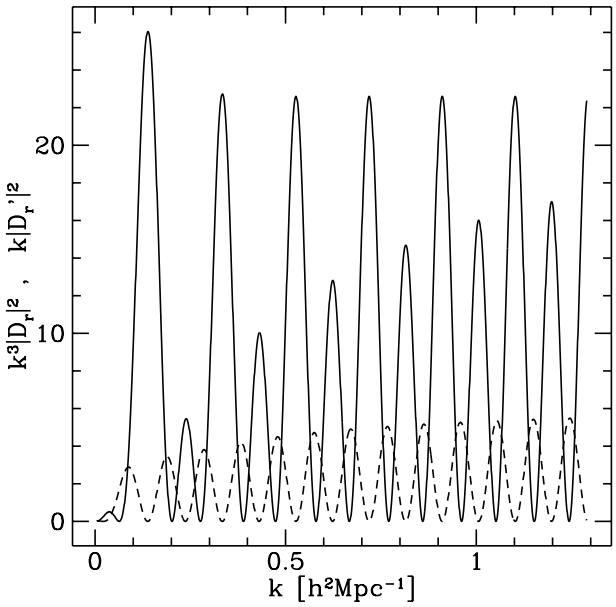

Figure 1: The dimensionless power spectra, $k^3|D_r|^2$ (solid line) and $k|D_r'|^2$ (dashed line) in units of $(A\epsilon)^2$, are shown as functions of k. These are exactly the quantities which enter in the expression for the C_ℓ's. We set $h = 0.5$, $\Omega_B = 0.05$ and $z_{rec} = 1100$.

Integrating Eq. (7), we obtain the Doppler contribution to the CMB anisotropies [*see*, Fig. 2]. For $\ell < 1000$, we find three peaks located at $\ell = 365$, $\ell = 720$ and $\ell = 950$. Silk damping, which we have not taken into account here, will substantially decrease the height of the second and even more that of the third peak. The integrated Sachs Wolfe effect, which also has been neglected, will shift the position of the first peak to somewhat larger scales, lowering ℓ_{peak} by (5 – 10)% and increasing its amplitude by less than 30%, as we argued above.

Our second result regards the amplitude of the first Doppler peak, for which we find

$$\ell(\ell+1)C_\ell \Big|_{\ell\sim 365} = 5\epsilon^2 \ . \tag{11}$$

As a consequence of the remark in footnote 4, the above numerical result has to be taken with a grain of salt. It is interesting to notice that the position of the first peak is displaced by $\Delta\ell \sim 150$ towards smaller angular scales than in inflationary models [6]. This is due to the fact that our solution represents a combination of the growing and decaying modes, and only once the perturbation enters the horizon and the source term becomes negligible, the decaying mode starts to decay. This is manifest in the difference in the growth of super–horizon perturbations, which is $D_r \propto t^{3/2}$ in our case, and $D_r \propto t^2$ for inflationary models, where on all scales only the growing mode is present.

One may understand the height of the first peak from the following analytic estimate: matching the sub–horizon with the super–horizon solutions of Eq. (5), in the matter dominated era, one finds $D_c \sim -0.4A\epsilon(k/2\pi)^{1/2}t^2$. From Eq. (4) we then obtain in this limit $D_r \approx A\epsilon k^{-3/2}$. Plugging this latter value into Eq. (7) we get roughly $\ell(\ell+1)C_\ell \sim (A\epsilon)^2$ for the height of the first peak. This agrees, within a factor 2 with the numerical result given in Eq. (11).

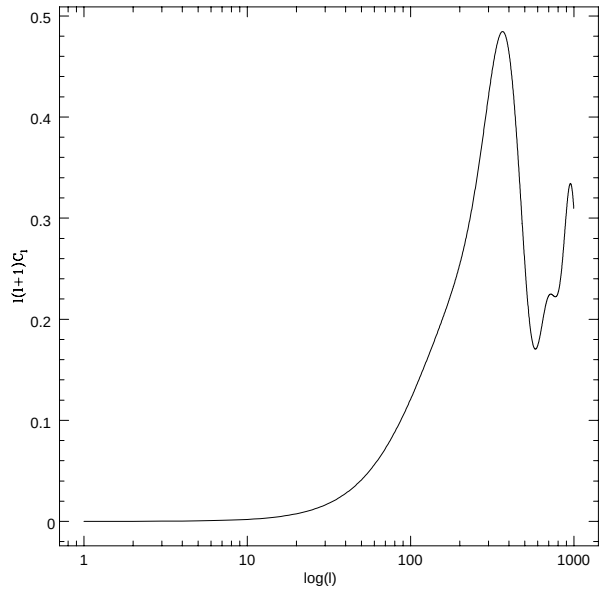

Figure 2: The angular power spectrum for the Doppler contribution to the CMB anisotropies is shown in units of ϵ^2. We set cosmological parameters $h = 0.5$, $\Omega_B = 0.05$ and $z_{rec} = 1100$

Let us now compare our value for the Doppler peak with the level of the SW plateau. Unfortunately, the numerical value for the SW amplitude is uncertain within a factor of about 2, which leads to a factor 4 uncertainty in the SW contribution to the power spectrum: Refs. [7, 8] and Ref. [9] find respectively

$$\ell(\ell+1)C_\ell \Big|_{SW} \sim 2\epsilon^2 \quad \text{and} \quad \ell(\ell+1)C_\ell \Big|_{SW} \sim 8\epsilon^2. \tag{12}$$

According to Refs. [7, 8], the Doppler peak is a factor of ~ 3.4 times higher than the SW plateau, whereas it is only about 1.5 times higher if the result found in [9] is assumed. (We allow for about 30% of the SW amplitude to be added in phase to the Doppler amplitude of $\sim 2.24\epsilon$, according to Eq. (11)). Clearly, improved numerical simulations or analytical approximations are needed to resolve this discrepancy. However, it is apparent from Eqs. (11) and (12) that the Doppler contribution from textures is somewhat smaller than for generic inflationary models.

We believe that our results are basically valid for all global defects. This depends crucially on the $1/\sqrt{t}$ behavior of $(\phi')^2$ on large scales (cf. Eq. (6)), which is a generic feature of global defects: on super–horizon scales, $(\phi')^2(k)$ represents white noise superimposed on the average given by $(\phi')^2(k=0) \propto \sqrt{V}/t^2$. Since there are $N = V/t^3$ independent patches in a simulation volume V, the amplitude of $(\phi')^2(k)$ is proportional to $\sqrt{V}/(t^2\sqrt{N}) \propto 1/\sqrt{t}$. (Notice that this argument does not apply for local cosmic strings.)

Based on our analysis, we conclude that if the existence of Doppler peaks is indeed confirmed and if the first peak is positioned at $\ell < 300$, *then* global topological defects are ruled out. On the other hand, if the first Doppler peak is positioned at $\ell \sim 350$ and if its amplitude is lower than the one predicted for standard inflationary models, global topological defects are strongly favored if compared to the latter. (There are however non–generic, open, tilted inflationary models which might

reproduce a similar signature in the CMB angular power spectrum). To our knowledge this is the first clear fingerprint within present observational capabilities, to distinguish among these two competing models of structure formation.

As a future work, we aim to model with better accuracy the global scalar field ϕ during both the radiation and the matter dominated era, as well as to include the SW effect and the photon diffusion. This will allow us to better estimate the amplitude of the first Doppler peak and to investigate secondary peaks.

As we were completing our work, a preprint[12] on the same issue, but following a different approach, came to our attention. The authors calculate the Doppler peaks from cosmic textures in the synchronous gauge. They include the Sachs Wolfe contribution into the analysis, but they need more of the uncertain modeling of the defect stress energy tensor. Even though we basically agree with the shape and position of their Doppler peaks, we obtain a somewhat smaller amplitude.

Acknowledgement
We thank Leandros Perivolaropoulos, who participated in the beginning of this project and Mark Hindmarsh, for helpful discussions and in particular for his skills with MATLAB. One of us (R.D.) acknowledges stimulating discussions with Neil Turok. A.G. thanks Nuno Antunes and Dennis Sciama for encouragement, the Institut für Theoretische Physik, Zürich for hospitality and The British Council for partial financial support. This work was partially supported by the Swiss NSF.

References

[1] P.J. Steinhard, *Class. Quantum Grav.* **10**, S33, (1993).

[2] T.W.B. Kibble, *Phys. Rep.* **67**, 183 (1980).

[3] R.K. Sachs and A.M. Wolfe, *Astrophys. J.* **147**, 73 (1967).

[4] R. Durrer, *Fund. of Cosmic Physics* **15**, 209 (1994).

[5] H. Kodama and M. Sasaki, *Prog. Theor. Phys. Suppl.* **78**, 1 (1984).

[6] N. Sugiyama, Preprint astro-ph/9412025 (1994).

[7] D. Bennett and S.H. Rhie, *Astrophys. J.* **406**, L7 (1993).

[8] U.–L. Pen, D.N. Spergel and N. Turok, *Phys. Rev.* **D49**, 692 (1994).

[9] R. Durrer and Z.H. Zhou, in preparation.

[10] N. Turok, *Phys. Rev. Lett.* **63**, 2625 (1989).

[11] A. Albrecht et al., Preprint, astro-ph/9505030.

[12] R.G. Crittenden and N. Turok, *Phys. Rev. Lett.* **75**, 2642 (1995).